Imaging parameter effects in apparent diffusion coefficient determination of magnetic resonance imaging

著者	Ogura Akio, Hayakawa Katsumi, Miyati Tosiaki, Maeda Fumie
journal or publication title	European Journal of Radiology
volume	76
number	2
page range	162-166
year	2010-01-01
URL	http://hdl.handle.net/2297/19223

doi: 10.1016/j.ejrad.2009.06.031

Imaging Parameter Effects in Apparent Diffusion Coefficient Determination of Magnetic Resonance Imaging

Akio Ogura, MS[1,2)]
Katsumi Hayakawa, MD [1)]
Tosiaki Miyati, PhD, DMSc [2)]
Fumie Maeda, RT [1)]

1) Department of Radiology, Kyoto City Hospital
2) Graduate School of Medical Science, Kanazawa University

Corresponding Author: Akio Ogura
Department of Radiology, Kyoto city hospital
1- 2, Higashitakada-cho, Mibu, Nakagyo-ku, Kyoto, JAPAN
TEL: +8175-311-5311(2183)
E-mail address: a-ogura@mbox.kyoto-inet.or.jp

Running Title: Imaging parameter effects in ADC

Abbreviated Title Page

Imaging Parameter Effects in Apparent Diffusion Coefficient Determination of Magnetic Resonance Imaging

Abstract

Purpose: Although an apparent diffusion coefficient (ADC) value is often used for differential diagnosis of tumours, it varies with scanning parameters. The present study was performed to investigate the influence of imaging parameters, *i.e.*, b value, repetition time (TR) and echo time (TE), on ADC value.

Methods: The phantoms were scanned using diffusion weighted imaging (DWI) with changing b values ($b = 0 – 3000$ s/mm^2), TR and TE to determine the influence on ADC. Moreover, ADC of the brain in normal volunteers was determined with varying b values ($b = 0 – 1000$ s/mm^2).

Results: Diffusion decay curves were obtained by biexponential fitting in all phantoms. The points where fast and slow components of the biexponential decay crossed were called turning points. The b values of turning points that crossed from the biexponential curve were different in each phantom. The b values of turning points depended on ADC of fast diffusion component. When ADC is calculated using two b values of front and back for the turning point, the ADC value may be different. Therefore, it was necessary to perform calculations by b value until the turning point to obtain the ADC value of the fast component. In addition, $b \geq 100$ was recommended to avoid the influence of perfusion by blood. Furthermore, the choice of long TR and short TE was effective for accurate measurement of ADC.

Conclusion: It is important to determine the turning point for measuring ADC.

Key words: turning points, apparent diffusion coefficient, biexponential decay

1. Introduction

Diffusion weighted images (DWI) obtained on magnetic resonance imaging (MRI) are useful for diagnosis of acute cerebral stroke. DWI is often used for examination of the human body because an echo planar imaging sequence with parallel imaging yields excellent image quality (1 – 13). Body DWI may allow rough differential diagnosis of tumours and is useful in examinations to find tumours. The apparent diffusion coefficient (ADC) is used frequently in differential diagnosis. It has been reported that DWI has the potential to differentiate between benign and malignant tumours (14 – 22). On the other hand, some investigators have reported that because ADC values of benign tumours and malignant tumours overlap, they are therefore not useful to differentiate between bulk benign and malignant tumours (23). In these cases, it is problematic that the ADC value varies with the scanning parameters. This leads to serious problems when ADC is used to distinguish a tumour. In addition, use of ADC value with an error may lead to wrong conclusions. Therefore, we reviewed how ADC value varies with scanning parameters, how to obtain ADC with high precision and points to which attention should be paid.

The purpose of this study was to identify the scanning parameters to obtain ADC value measurement with a high degree of precision.

2. Materials and methods

2-1. Phantom study

2-1-1. Influence of b value

The phantoms were scanned with various b values (b = 0 – 3000 s/mm^2) to determine the influence of the b value of the motion probing gradient (MPG) on signal intensity of DWI. Five types of phantom (agarose 1 g, 3 g, 4 g and 5 g in 100 mL of hot water and 100 mL of liquid detergent in bottles) were fixed in a water tank.

T1 and T2 values of each phantom are shown in Table 1.

Scanning parameters were TR/TE with 8000/100 ms with spin-echo type

single-shot echo planar imaging (EPI), matrix size, 128 × 128; field of view, 20 × 20 cm; number of signals averaged, 20; slice thickness, 6 mm. All studies were performed with a 1.5 T superconductive unit (Magnetom Symphony; Siemens, Erlangen, Germany) using an 8-ch head coil with sensitivity revision. The signal intensity value of each phantom image was measured with manually defined regions of interest 1 cm in diameter. ADC was calculated from the signal intensities of two points of the b value with the following equation:

$$ADC = \ln (S1/S2) / (b2 - b1) \quad (1)$$

where S is the signal intensity and b is the b value.

ADC was calculated from the DWI signal on b = 0 and another point (b = 0 – 3000 s/mm^2).

2-1-2. Influences of TR and TE

The phantom was scanned with various TR (TR = 1000 – 8000 ms) and TE of 100 ms of EPI sequence to review the influence of TR. ADC was calculated from the signals of DWI on b = 0 and 1000 s/mm^2.

In addition, the phantom was scanned with various TE (TE = 50 – 400 ms) and TR of 8000 ms of EPI sequence to review the influence of TE. ADC was calculated from the signals of DWI on b = 0 and 1000 s/mm^2.

2-2. Human brain study

The institutional review board approved the study design and review of volunteer records and images. The brains of three human subjects who provided informed consent were scanned on DWI with various MPG (b = 0 – 1000 s/mm^2) to review the accuracy of ADC value in the living body. Scanning parameters were TR/TE of 8000/100 ms, slice thickness of 6 mm, field of view of 22 cm and a matrix of 128 × 256 with EPI. Each ADC was calculated with b values of two adjacent points, with manually defined regions of interest in the white matter and grey matter (Figure 1).

3. Results

The logarithms of DWI signal intensities with b = 0 – 3000 s/mm^2 are plotted in Figure 2. In all phantoms, the signal intensity deteriorated as b value increased, indicated by two straight lines on the logarithmic scale. That is, diffusion decay curves were obtained from the biexponential in all phantoms. The points where fast and slow components of the biexponential decay crossed were called turning points (Figure 3).

The positions of the turning points were different in each phantom in Figure 2. Figure 4 shows the relations between the ADC value of the fast component (the first straight line part) and the b value of the turning point. With increases in ADC, the b value of the turning point tended to fall. Therefore, the b value of the turning point for the biexponential was dependent on ADC.

The ADC values calculated from two points between b = 0 and the turning point were almost the same, but the ADC values calculated from two points with b = 0 and large b values greater than the turning points were decreased, as shown in Figure 5.

Figure 6 shows the ADC value when TR changed from 1000 to 8000 ms in the scanning parameter of DWI. The ADC value was different in a gel consisting of dissolved agarose solution from TR = 1000 to 3000 ms.

Figure 7 shows the ADC value when TE changed from 50 to 400 ms in the scanning parameter of DWI. In this case, there was no significant difference in solution. In a gel consisting of 3 – 5 g of agarose in solution, no difference was seen at TE = 50, 100 ms, but a drop in ADC was seen with increases in TE.

The calculated ADC values for different b values in DWI in the human brain are shown in Figure 8. The ADC values decreased at b = 0 and 100 s/mm^2. In addition, the ADC values decreased with increases in b value.

The ADC values calculated for b = 0 and high b value and for b = 100 s/mm^2 and high b value in the human brain are shown in Figure 9. Calculated ADC value was stable for b = 100 s/mm^2 and high b value.

4. Discussion

In all phantoms, the signal intensity deteriorated with increases in b value as shown in Figure 2. The decay curves were best fit with the biexponential function. In general, biexponential decay occurs due to intra- and extracellular diffusion (24, 25). Other investigators reported that the fast and slow diffusion components responsible for the biexponential decay are attributable to water and lipid protons using dairy cream (26, 27). In this study, the biexponential decay was seen in the agarose phantom. Although interesting, the origin of the biexponential is still unclear.

The positions of turning points where fast and slow components crossed were different in each phantom. With a rise in ADC of the fast component, the b value of the turning point tended to deteriorate as shown in Figure 4. The b value of turning point of the biexponential was dependent on ADC.

If ADC is calculated by two points, the b value of the front and back for the turning point, the ADC value is different for fast and slow components because ADC is calculated from the slope of the straight line between two points (see Figure 3). In fact, this can be seen clearly in Figure 4.

Calculations should be performed using b values up to the turning point to obtain the ADC value of the fast component.

In addition, as a scanning parameter of DWI, shortened TR leads to dependence on the ADC value for some materials as shown in Figure 6. Table 1 shows T1 and T2 values of the phantom. The material with long T1 value influenced the ADC value. That is, for a material with long T1 value, errors are produced in the ADC value by setting a short TR. However, there were no changes for a long TR. Similarly, ADC deteriorated with increases in TE for a material with short T2 value. However, there were no changes for short TE. Therefore, the scanning parameter of DWI with long TR and short TE can reduce measurement error.

The signal intensity of DWI deteriorated at b = 0 in scanning of the human brain as shown in Figure 8. This was thought to be under the influence of perfusion. It has been reported previously that the diffusion signal is

influenced by perfusion with small b value, which was confirmed by this result.

Therefore, a stable ADC value is obtained using a small b value of about 100 s/mm^2 and a large b value before the turning point (see Figure 9).

5. Conclusions

Recently, DWI and ADC have become important tools in surveying and discrimination of tumours. Many studies are now performed using ADC value to distinguish tumours. On the other hand, the ADC value varies with scanning parameters of DWI. Use of an ADC value with an error may lead to wrong conclusions.

Therefore, the present study was performed to investigate the scanning parameters to obtain high precision in ADC measurement. It is necessary to use b values smaller than the turning point so that signal intensity of DWI decays by biexponential fitting for b value. Therefore, it is important to determine the turning point for measurement of ADC.

A value of $b \geq 100$ s/mm^2 is recommended to avoid the influence of perfusion by blood. In addition, the choice of long TR and short TE was effective for highly precise measurement of ADC for considered T1 and T2 values of objects. It is possible to measure ADC with a high degree of precision by taking the above points into consideration.

References

1. Takahara T, Imai Y, Yamashita T, et al. Diffusion weighted whole body imaging with background body signal suppression (DWIBS): technical improvement using free breathing, STIR and high resolution 3D display; Radiat Med 2004;22: 275-282.

2. Nasu K, Kuroki Y, Nawano S, et al. Hepatic mrtastases: Diffusion weighted sensitivity-encoding versus SPIO-enhanced MR imaging; Radiology 2006;239: 122-130.

3.Moteki T, Ishizuka H. Diffusion-weighted EPI of cystic ovarian lesions:

evaluation of cystic contents using apparent diffusion coefficients; J.Magn .Reson.Imaging 2000;12: 1014-1019.
4.Moteki T, Horikoshi H, Endo K. Diffusion coefficient and signal intensity in endometrial and other pelvic cysts; Magn.Reson.Imaging 2002;20: 463-470.
5.Sato C, Naganawa S, Nakamura T, et al. Differentiation of noncancerous tissue and cancer lesions by apparent diffusion coefficient values in transition and peripheral zones of the prostate; J.Magn.Reson.Imaging 2005; 21: 258-262.
6.Shimofusa R, Fujimoto H, Akamoto H,et al. Diffusion-weighted imaging of prostate cancer; J Compt.Assist.Tomogr 2005;29: 149-153.
7.Naganawa S, Sato C, Kumada H, et al. Apparent diffusion coefficient in cervical cancer of the uterus: comparison with the normal uterine cervix; Eur Radiol 2005;15: 71-78.
8.K Hosseinzadeh, SD Schwarz. Endorectal diffusion-weighted imaging in prostate cancer to differentiate malignant and benign peripheral zone tissue; J.Magn.Reson.Imaging 2004;20: 654-661.
9. Naganawa S, Kawai H, Fukatsu H, et al. Difusion-weighted imaging of the liver: Technical challenges and prospects for the future; Magnetic Resonance in Medical Sciences 2005;4: 175-186.
10.MD Pickles, P Gibbs, M Sreenivas, et al. Diffusion-weighted imaging of normal and malignant prostate tissue at 3T; J.Magn.Reson.Imaging 2006;23: 130-134.
11.M Koinuma, I Ohashi, K Hanafusa, et al. Apparent diffusion coefficient measurements with diffusion-weighted magnetic resonance imaging for evaluation of hepatic fibrosis; J.Magn.Reson.Imaging 2005;22: 80-85.
12.Sun XJ, Quan XY, Huang FH, et al. Quantitative evaluation of diffusion-weighted magnetic resonance imaging of focal hepatic lesions; World J Gastroenterol 2005;11 (41):6535-6537.
13.T Yoshikawa, H Kawamitsu, DG Mitchell, et al. ADC measurement of abdominal organs and lesions using parallel imaging technique; AJR 2006;187: 1522-1530.

14.S Higano, Xia Yun, T kumabe, et al. Malignant astrocystic tumors: clinical importance of apparent diffusion coefficient in prediction of grade and prognosis; Radiology 2006;241(3):839-846.
15.Bulakbasi N, Guvenc I, Onguro O, et al.The added value oof the apparent diffusion coefficient calculation to magnetic resonance imaging in the differentiation and grading of malignant brain tumors; J Comput Assist Tomogr 2004;28(6): 735-746.
16.Muti M, Aprile I, Principi M, et al. Study on the variations of the apparent diffusion coefficient in areas of solid tumor in high grade gliomas; Magn Reson Imaging 1999;20(9):53-60.
17. Park Mi Jung, Cha Eun Suk, Kang Bong Joo, et al. The role of diffusion-weighted imaging and the apparent diffusion coefficient (ADC) values for breast tumors; Korean journal of radiology 2007; 8(5):390-396.
18. Yerli H, Agildere A M, Aydin E, at al. Value of apparent diffusion coefficient calculation in the differential diagnosis of parotid gland tumors; Acta radiological 1987;48 (9): 980-987.
19. Matsushima N, Maeda M, Takamura M, et al. Apparent diffusion coefficients of benign and malignant salivary gland tumors; Comparison to histopathological findings. Journal of neuroradiology 2007; 34 (3):183-189.
20. desouza N M, Reinsberg S A, Scurr E D, et al. Magnetic resonance imaging in prostate cancer: the value of apparent diffusion coefficients for identifying malignant nodules; British journal of radiology 2007; 80(950):90-95.
21. Eida S, Sumi M, Sakihama N, et al. Apparent diffusion coefficient mapping of salivary gland tumors: prediction of the benignancy and malignancy; AJNR 2007;28 (1): 116-121.
22.Nakayama T, Yoshimitsu K, Irie H, et al. Diffusion-weighted echo-planar MR imaging and ADC mapping in the differential diagnosis of ovarian cystic masses: usefulness of detecting keratinoid substances in mature cystic teratomas; JMRI 2005; 22 (2): 271-278.
23. Matsushima N, Maeda M, Takamura M, et al. Apparent diffusion coefficients of benign and malignant salivary gland tumors. Comparison to

histopathological findings; J neuroradiology2007; 34: 183-189.
24.Schwarcz A, Bogner P, Meric P, et al. The existence of biexponential signal decay in magnetic resonance diffusion-weighted imaging appears to be independent of compartmentalization; Magn Reson in Medicine2004; 51: 278-285.
25.Inglis BA, Bossart EL, Buckley DL, et al. Visualization of neural tissue water compartments using biexponential diffusion tensor MRI; Magn Reson in Medicine2001; 45: 580-587.
26. Ababneh Z, Haque M, Maier SE, et al. Daily cream as a phantom material for biexponential diffusion decay; MAGMA 2004; 17: 95-100.
27. Sehy JV, Ackerman IJ, Neil JJ. Evidence that both fast and slow water ADC components arise from intracellular space; Magn Reson Med2002; 48: 765-770.

Figure legends

Figure 1: Regions of interest of white matter and grey matter in the human brain used to calculate ADC.

Figure 2: Logarithmic signal intensity with b = 0 – 3000 s/mm^2 in the phantoms.

Figure 3: The signal intensity of DWI deteriorated as b value increased. This rate of decrease is indicated by two straight lines (fast and slow components) on the logarithmic scale. The points where fast and slow components of the biexponential decay crossed were called turning points.

Figure 4: Relation of ADC value of first component and b value of turning point of the biexponential. The b value of the turning point decreased with increases in ADC.

Figure 5: ADC values were calculated for different b values. ADC was stable using a b value before the turning point, but ADC deteriorated when the b value was after the turning point.

Figure 6: Dependence of the ADC value on different TR in EPI-DWI sequence. ADC value varied with TR by material.

Figure 7: Dependence of the ADC value on different TE in EPI-DWI sequence. ADC value varied with TE by material.

Figure 8: ADC values calculated with different b values in the white matter and gray matter of the human brain. The b value calculated from b = 0, 100 became comparatively small.

Figure 9: ADC values calculated with different b values in the white matter

and grey matter of the human brain. ADC value was stable when having turned b value of small part into 100 s/mm^2.

Table 1: T1 and T2 values of the phantom materials used this experiment.

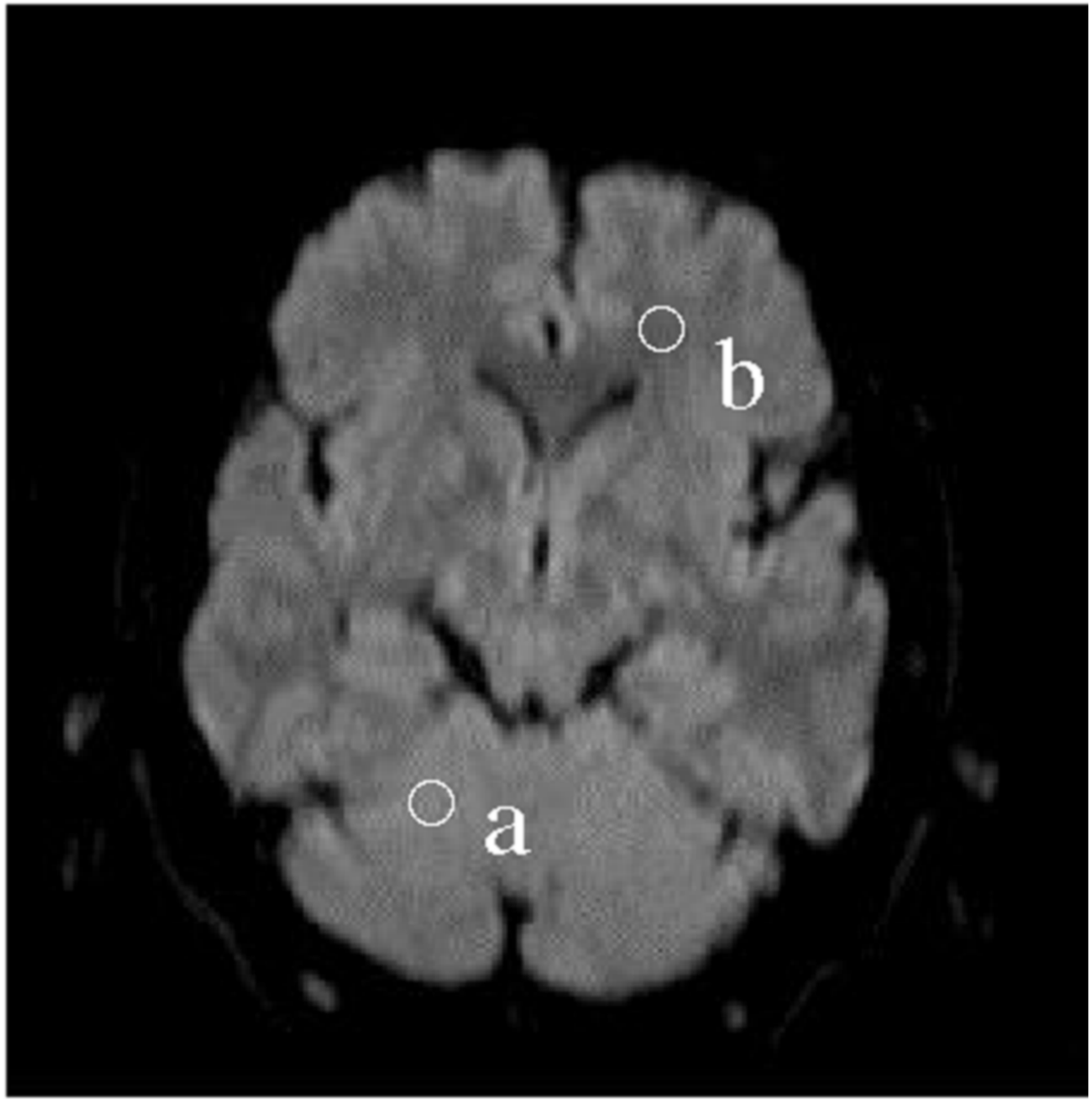

Fig.1

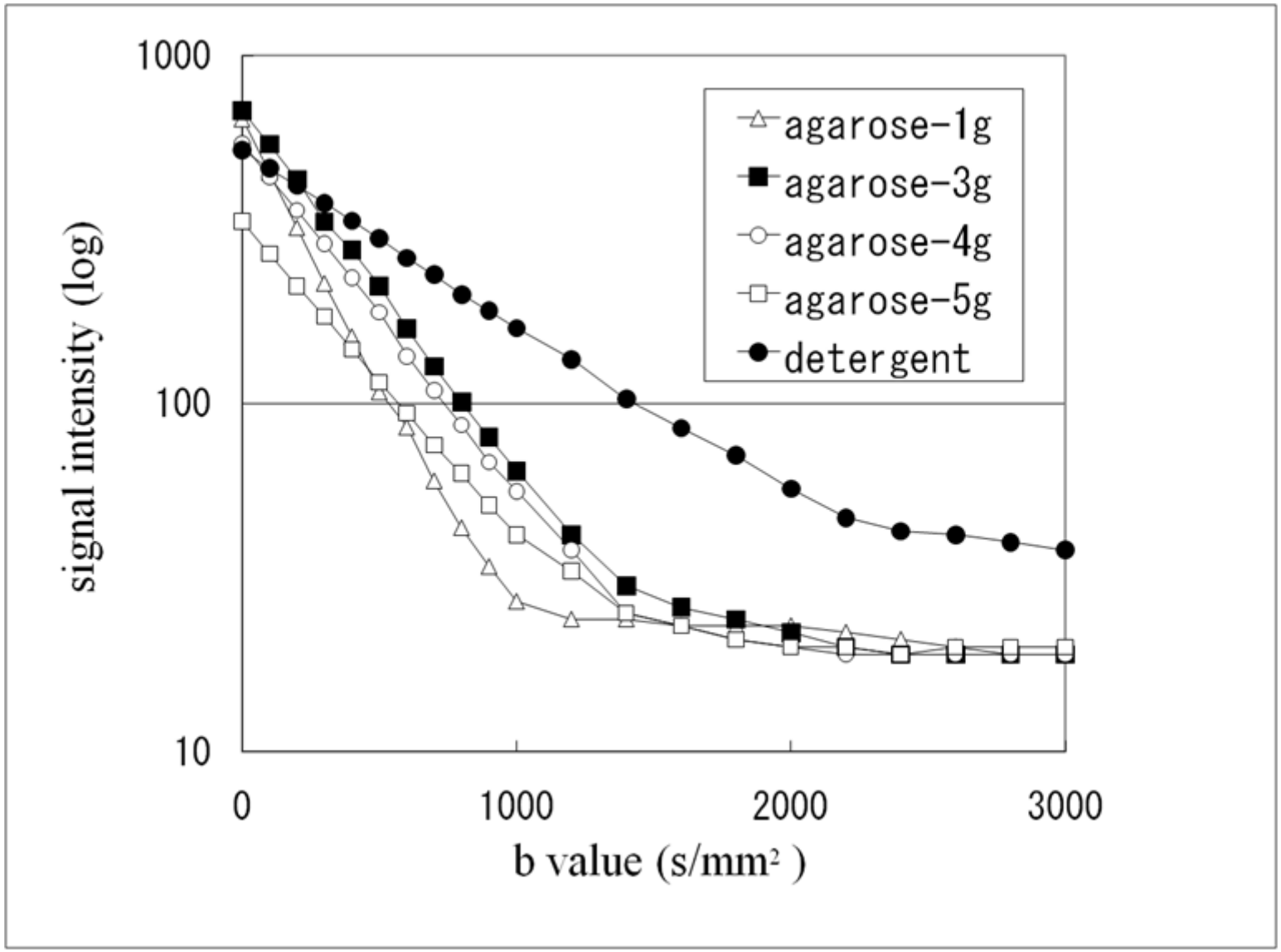
1000
100
10
signal intensity (log)
0
1000
2000
3000
b value (s/mm²)
agarose-1g
agarose-3g
agarose-4g
agarose-5g
detergent

Fig.2

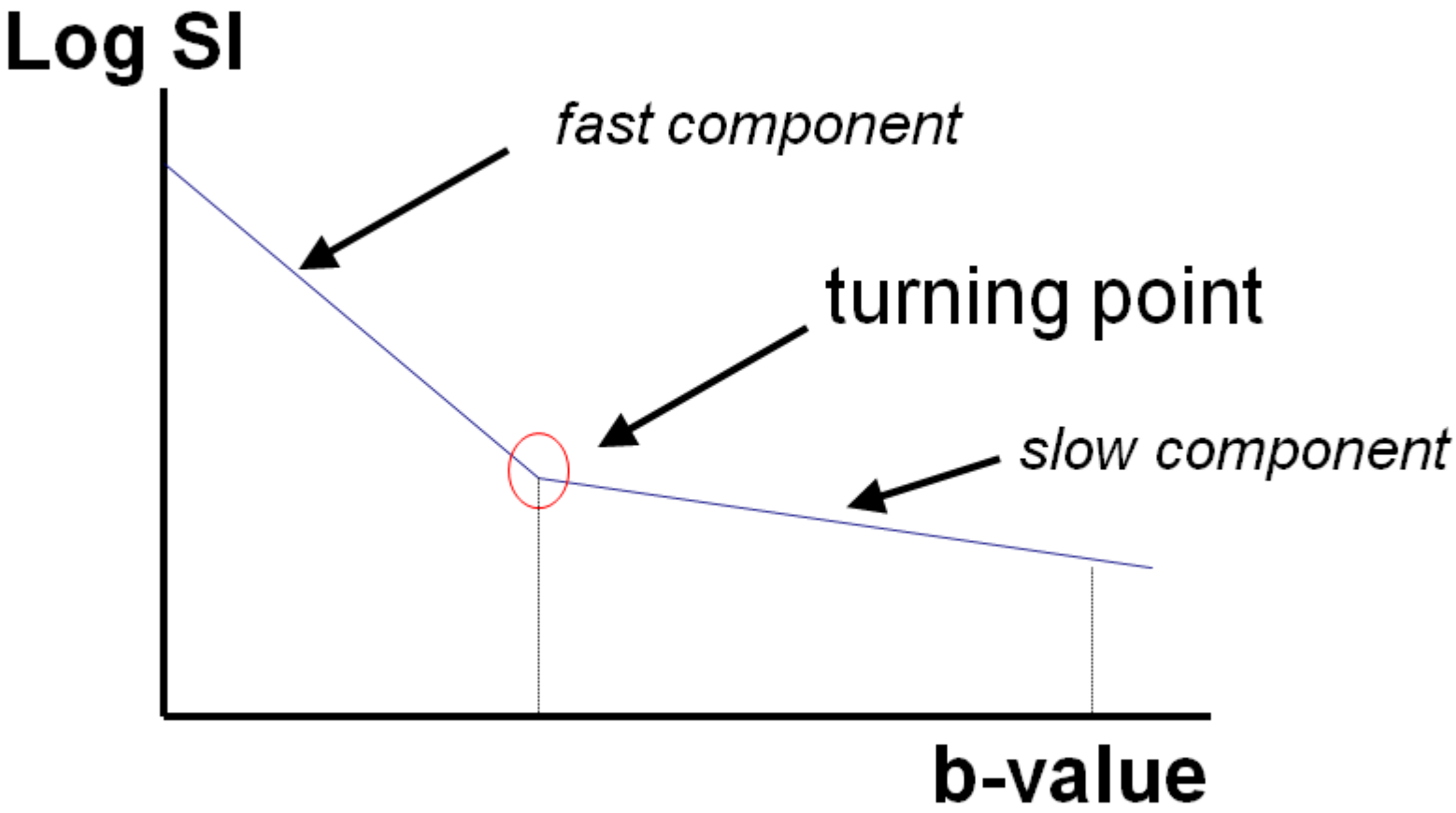

Fig.3

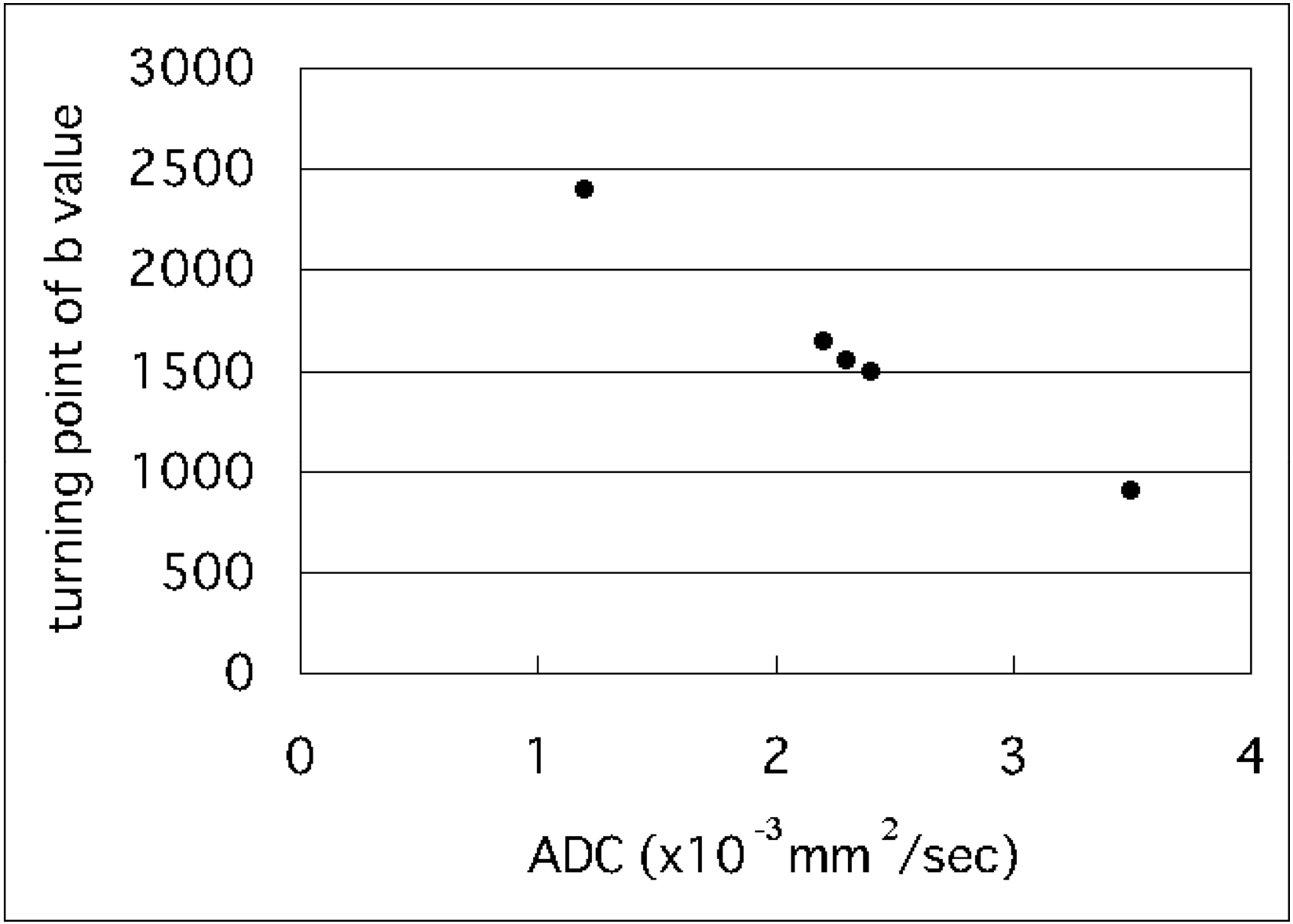
3000
2500
2000
1500
1000
500
0
turning point of b value
0
1
2
3
4
ADC (x10 -3 mm 2 /sec)

Fig.4

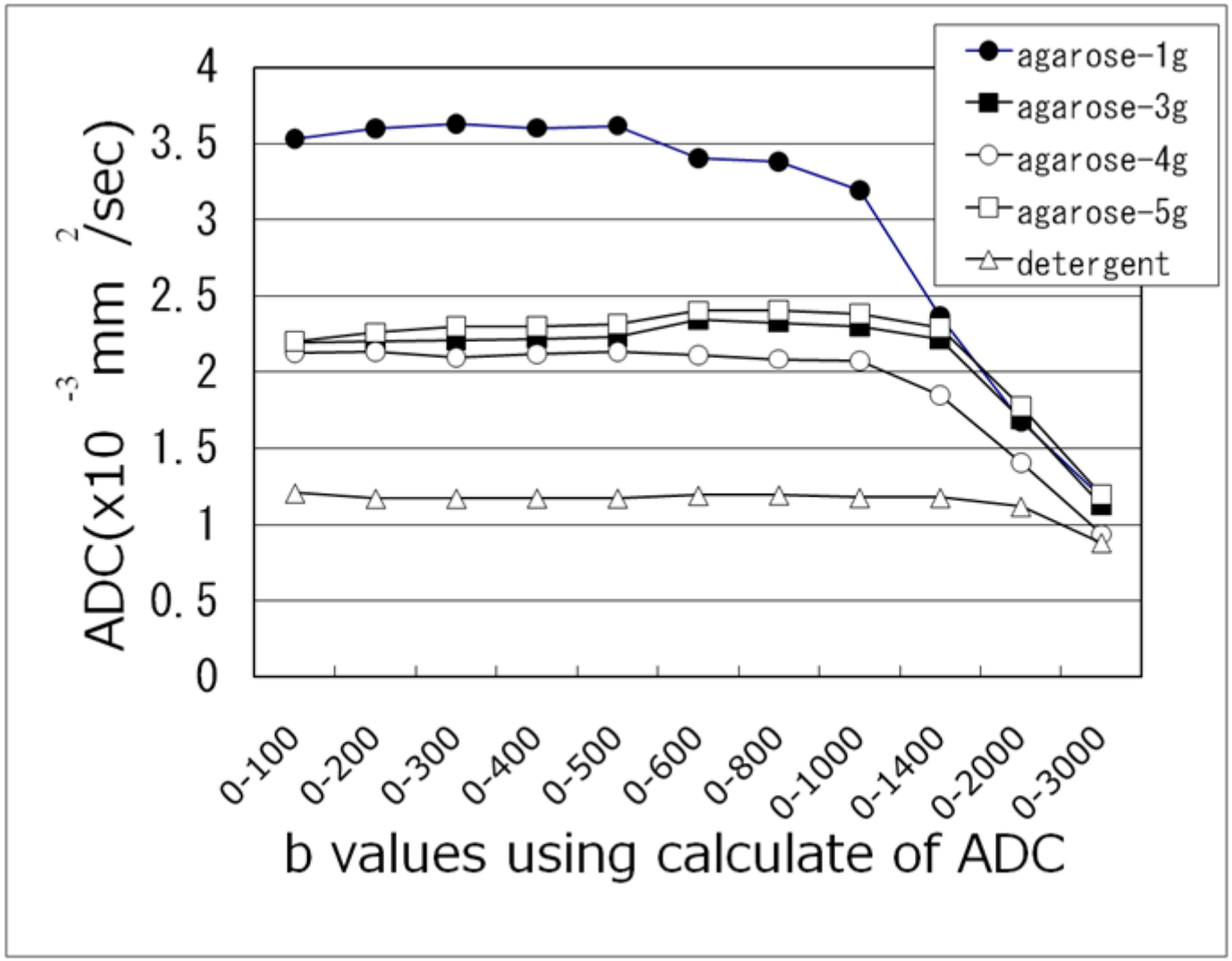
agarose-1g
agarose-3g
agarose-4g
agarose-5g
detergent
ADC(x10 -3 mm 2 /sec)
4
3.5
3
2.5
2
1.5
1
0.5
0
0-100
0-200
0-300
0-400
0-500
0-600
0-800
0-1000
0-1400
0-2000
0-3000
b values using calculate of ADC

Fig.5

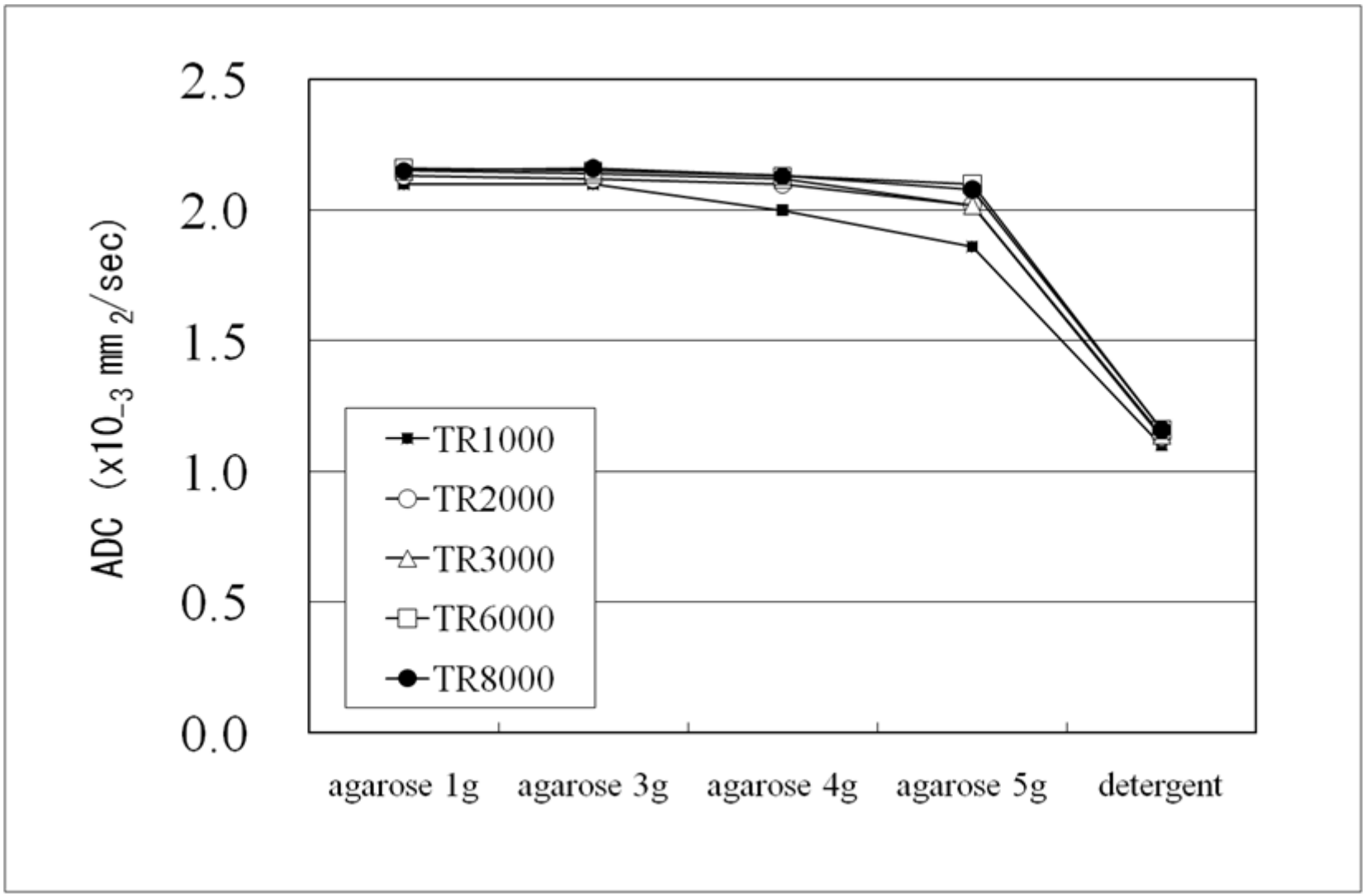
2.5
2.0
1.5
1.0
0.5
0.0
ADC (x10-3 mm2/sec)
TR1000
TR2000
TR3000
TR6000
TR8000
agarose 1g
agarose 3g
agarose 4g
agarose 5g
detergent

Fig.6

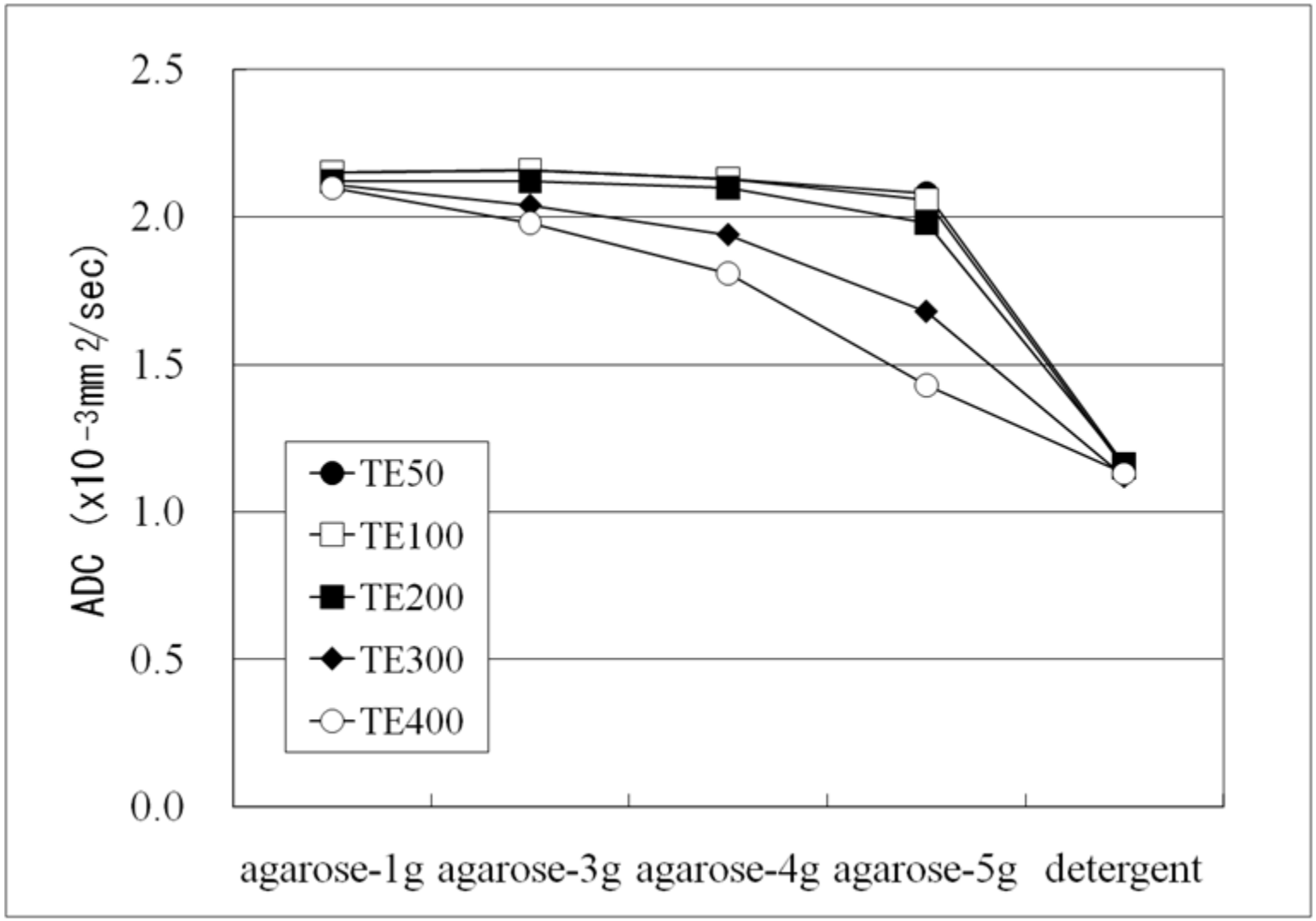
2.5
2.0
1.5
1.0
0.5
0.0
ADC (x10-3mm 2/sec)
TE50
TE100
TE200
TE300
TE400
agarose-1g
agarose-3g
agarose-4g
agarose-5g
detergent

Fig.7

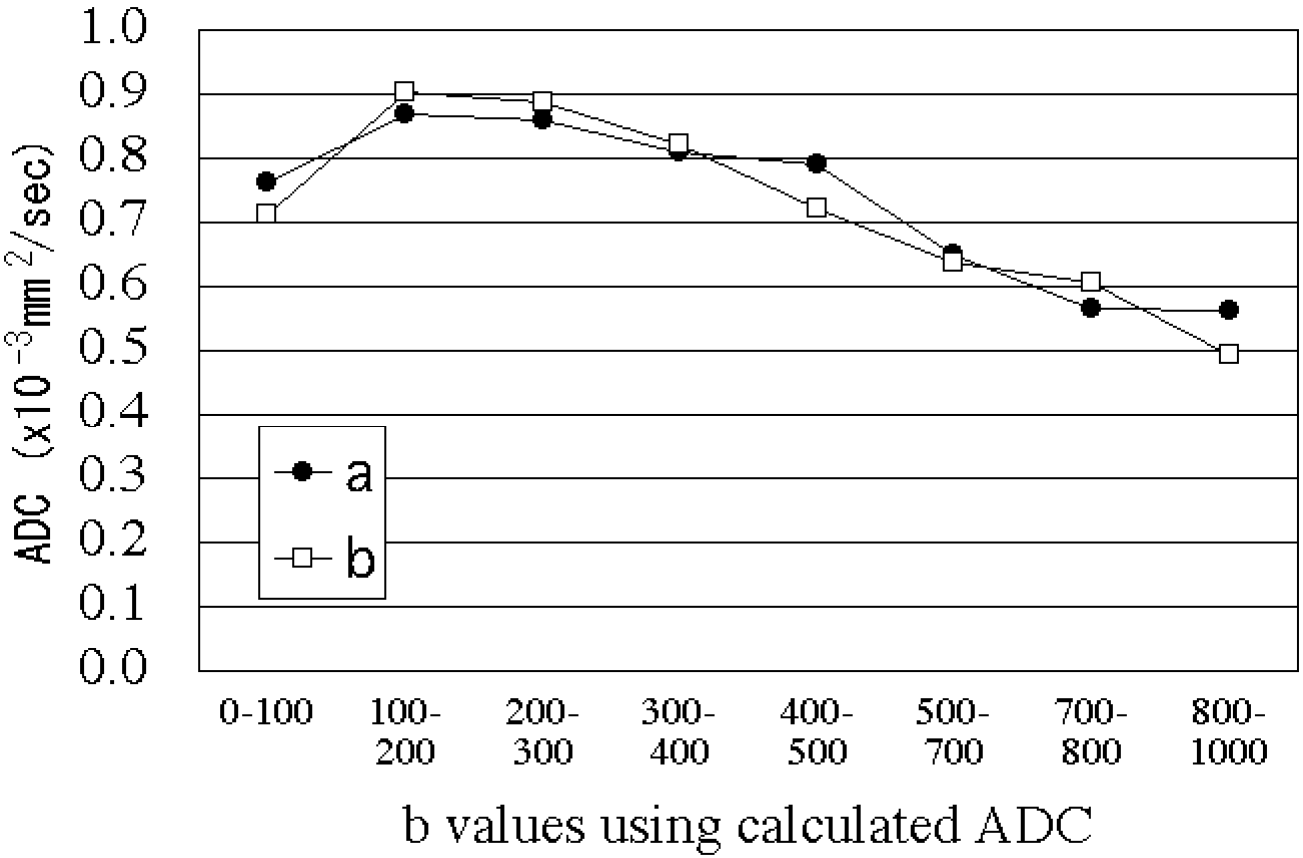
1.0
0.9
0.8
0.7
0.6
0.5
0.4
0.3
0.2
0.1
0.0
ADC (x10 -3mm 2/sec)
a
b
0-100
100-200
200-300
300-400
400-500
500-700
700-800
800-1000
b values using calculated ADC

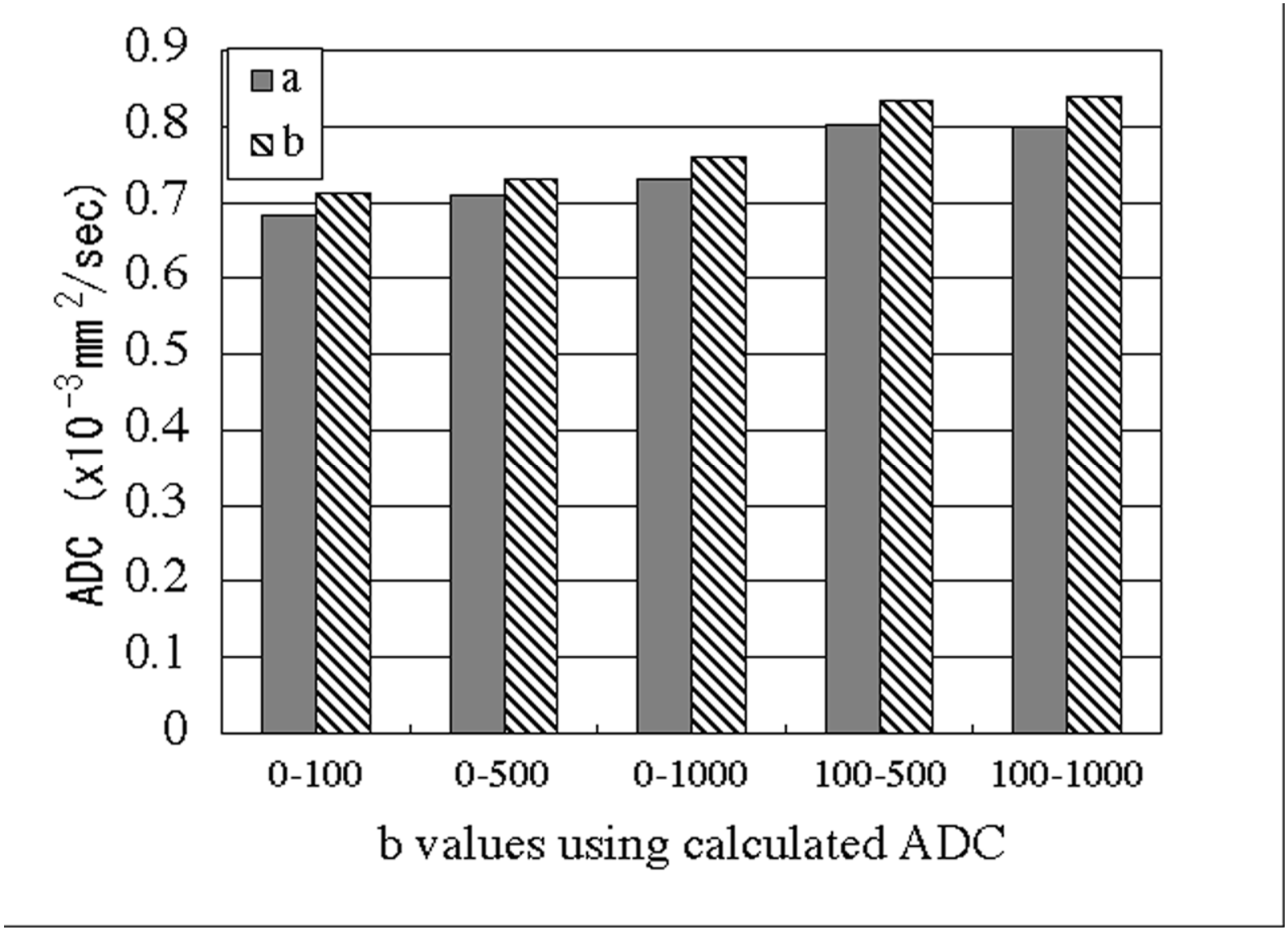
0.9
0.8
0.7
0.6
0.5
0.4
0.3
0.2
0.1
0
a
b
ADC (x10^{-3}mm^2/sec)
0-100
0-500
0-1000
100-500
100-1000
b values using calculated ADC

	T1(msec)	T2(msec)
agarose 1g	2431	172
agarose 3g	2796	88
agarose 4g	2917	70
agarose 5g	3039	60
detergent	2115	170